Atherosclerosis 288 (2019) 124–136

Contents lists available at ScienceDirect

Atherosclerosis

journal homepage: www.elsevier.com/locate/atherosclerosis

RhoGDI stability is regulated by SUMOylation and ubiquitination via the AT1 receptor and participates in Ang II-induced smooth muscle proliferation and vascular remodeling

Fan Dai[a,1], Yan Qi[a,1], Wei Guan[a], Guoliang Meng[a], Zhaoguo Liu[a], Ting Zhang[b], Wenjuan Yao[a,*]

[a] School of Pharmacy, Nantong University, 19 QiXiu Road, Nantong, 226001, China
[b] Save Sight Institute, The University of Sydney, NSW, 2000, Australia

HIGHLIGHTS

- The stability of RhoGDI1 and RhoGDI2 participates in AngII-mediated smooth muscle phenotypic transformation and vascular remodeling.
- SUMOylation and ubiquitination reciprocally regulate RhoGDI stability via the AT1 receptor.
- RhoGDI targeted degradation may provide a novel approach for treatment of vascular remodeling.

ARTICLE INFO

Keywords:
RhoGDI
SUMOylation
Ubiquitination
Angiotensin II
Vascular remodeling

ABSTRACT

Background and aims: The physiological role of Rho-specific guanine nucleotide dissociation inhibitor (RhoGDI) in vascular remodeling remains unknown. We investigated the function of RhoGDI in angiotensin II (Ang II)-induced vascular remodeling in cultured human aortic vascular smooth muscle cells (HA-VSMCs) and in an Ang II-infusion vascular remodeling mouse model.

Methods: For *in vitro* assays of HA-VSMCs, proliferation was assessed by BrdU and EdU assays and immunofluorescence analysis of ki-67 expression. RhoGDI1 and RhoGDI2 function and expression were assessed by RNAi, Western blotting and real-time RT-PCR. RhoGDI ubiquitination and SUMOylation levels were evaluated by co-immunoprecipitation and Western blotting. The functions of proteosomal-mediated degradation, ubiquitination, SUMOylation and Ang II receptors were assessed using specific inhibitors. To evaluate the *in vivo* effects of Ang II and RhoGDI, H & E staining, Masson's trichrome staining, and immunostaining were employed.

Results: Ang II treatment of HA-VSMCs for 6 or 48 h promoted RhoGDI1 and RhoGDI2 protein degradation and reduced cell proliferation, which was reversed by proteosome inhibition. In contrast, treatment with Ang II for 12 or 24 h induced dose-dependent cell proliferation without affecting RhoGDI expression. RNA interference of either RhoGDI1 or RhoGDI2 blocked proliferation induced by 12 or 24 h treatment of Ang II. Moreover, Ang II-dependent degradation at 6 and 48 h correlated with RhoGDI ubiquitination and inversely correlated with RhoGDI SUMOylation and cell proliferation. Treatment with specific inhibitors suggests that ubiquitin and SUMO competitively bind to RhoGDI1 and RhoGDI2 to reciprocally regulate RhoGDI stability and HA-VSMC proliferation. Furthermore, inhibition of the Ang II receptor 1 (AT1 receptor), but not the Ang II receptor 2, blocked Ang II-dependent RhoGDI stabilization and proliferation at 12 and 24 h. In mice, Ang II infusion increased the intima-media thickness, collagen and myofiber production and VSMC proliferation, and these effects were shown to be dependent on RhoGDI1, RhoGDI2 and AT1 receptor. Ang II infusion exerted no significant effect on RhoGDI1 and RhoGDI2 protein levels, which were decreased after AT1 receptor inhibition.

Conclusions: Together, the results of this study reveal a novel mechanism by which Ang II regulates RhoGDI stability by SUMOylation and ubiquitination via AT1 receptor activation and thus affects VSMC proliferation and vascular remodeling.

* Corresponding author. Department of Pharmacology, School of pharmacy, Nantong University, 19 QiXiu Road, Nantong, 226001, Jiangsu, China.
E-mail address: yaowenjuan0430@aliyun.com (W. Yao).
[1] These authors contributed equally to this work.

https://doi.org/10.1016/j.atherosclerosis.2019.07.010
Received 25 January 2019; Received in revised form 20 June 2019; Accepted 11 July 2019
Available online 23 July 2019

1. Introduction

Vascular remodeling is implicated to be the pathophysiological basis of life-threatening cardiovascular diseases such as hypertension, atherosclerosis, and restenosis. It has been reported that the transition of vascular smooth muscle cells (VSMCs) from a contractile phenotype to a proliferative synthetic phenotype plays a critical role in vascular development and remodeling [1,2]. Angiotensin II (Ang II) activates signaling responses via its receptor and thereby mediates inflammation, proliferation, migration, and hypertrophy [3–5]. There is considerable evidence indicating that, under certain conditions, Ang II exhibits growth promoting effects and migration in VSMCs, which contributes to vascular remodeling in cardiovascular disease [6–8]. Unfortunately, it is still unclear which signaling pathway acts downstream of the Ang II receptors (AT1-R and AT2-R) to mediate HA-VSMC phenotypic modulation and neointima formation.

Rho specific guanine nucleotide dissociation inhibitor (RhoGDI) is critical for both homeostasis of Rho proteins and crosstalk between the family members [9]. It has been reported that depletion of RhoGDI1 or its yeast ortholog RDI1 results in almost complete degradation of RhoA, Rac1 and Cdc42 by the proteasome in eukaryotic cells [10]. There are three RhoGDI isoforms -RhoGDI1, RhoGDI2, RhoGDI3- and they play crucial roles in various cellular functions, such as proliferation and migration [10,11]. RhoGDI1 (also known as RhoGDIα or ARHGDIA) is the most abundant and distinctive member of the family and has been reported to be ubiquitously expressed [10]. RhoGDI2 (also known as RhoGDIβ, Ly-GDI, D4-GDI, or ARHGDIB) is usually highly expressed in hematopoietic cells, but has also been found in other cells such as cancer cells [11,12]. RhoGDI3 (also known as RhoGDIγ or ARHGDIG) is specifically expressed in the lungs, brain and testes, and usually at low levels [11,13]. In addition, many studies have shown that RhoGDI expression levels are severely altered in a range of cancers [14–17]. Recent studies have shown that RhoGDI protein is regulated by Ang II [18–20]; however, its function in VSMCs has not been demonstrated.

SUMOylation, a reversible post-translational modification by the small ubiquitin-like modifiers (SUMOs), participates in a variety of cellular processes, including DNA replication, transcription, cell cycle regulation, signal transduction and protein degradation [21–24]. There are five SUMO paralogues in mammals [25]. SUMO1–SUMO3 are ubiquitously expressed while the expression of SUMO4 and SUMO5 is restricted to specific tissues [26]. It has been reported that SUMOylation facilitates protein aggregation and activation by blocking its ubiquitin-dependent degradation pathways [27,28]. In addition, RhoGDI can be SUMOylated specifically at residue Lys-138, which is crucial for RhoGDI inhibition of cancer cell motility and invasion [29]. However, it remains unclear whether RhoGDI and its SUMOylation are involved in HA-VSMC phenotypic modulation and pathological vascular remodeling.

In the present study, we used an *in vitro* Ang II-mediated HA-VSMC proliferation model and an *in vivo* Ang II-infusion vascular remodeling model to investigate the effects of RhoGDI1 and RhoGDI2 on Ang II-induced HA-VSMC proliferation and vascular remodeling and to clarify the molecular mechanisms behind these effects.

2. Materials and methods

2.1. Materials

Ang II was obtained from MedChemExpress (#HY-B0202; State of New Jersey, USA). Fetal bovine serum (FBS; #F2442) and 4′, 6-Diamidino-2-phenylindole (DAPI; #28718-90-3) were purchased from Sigma Chemical Co. (St. Louis, MO, USA). Ginkgolic acid (GA, an inhibitor of the SUMOylation E1 enzyme) was purchased from ZZBIO CO., LTD (20,261-38-5; Shanghai, China). Total RNA Purification Kits were purchased from GeneMark (#TR01-150; Taichung, Taiwan). RevertAid First Strand cDNA Synthesis Kit (#K1622), GeneRuler 1 kb DNA Ladder (#SM0311), and Dream Taq PCR Master Mix (#K1071) were from Thermo Scientific (Shanghai, China). SiRNAs (Table 1) and primers (Table 2) were purchased from Biomics Biotechnologies (Nantong, China). MG132 (proteasome inhibitor; #S2619), candesartan (AT1 receptor inhibitor; #139481-59-7), PD123319 (AT2 receptor inhibitor; #130663-39-7), and PYR-41 (an inhibitor of ubiquitin-activating enzyme E1; CC7285) were from ChemCatch Co., Ltd (Shanghai, China). N-ethylmaleimide (NEM) was obtained from Sigma-Aldrich Chemical Co. (#128-53-0; St. Louis, MO, USA). Irbesartan (#HY-B0202) was purchased from MedChemExpress (NJ, USA). Anti-RhoGDI2 (ab181252), -SUMO1 (ab32058), -SUMO 2 + 3 (ab3742) and -α-SMA (ab124964) antibodies were all from Abcam (Cambridge, MA, USA). Primary antibody against GAPDH (#5174) was from Cell Signaling Technology (Beverly, MA, USA). RhoGDI1 (A1214), Ki-67 (A11390) and Ubiquitin (A3207) polyclonal antibodies were purchased from ABclonal (Wuhan, China). Peroxidase-conjugated AffiniPure Goat Anti-Rabbit IgG (H + L) was from Proteintech (SA00001-2; Chicago, IL, USA). Fluorescein (FITC)-conjugated AffiniPure Donkey Anti-Rabbit IgG (H + L) was from BBI Life Sciences (D110051; Hong Kong, China). Bromodeoxyuridine (BrdU) proliferation assay kits were purchased from Merck Millipore (#2750; Millipore, Billerica, MA, USA). Cell-Light™ EdU Apollo®567 In Vitro Imaging Kits (100T) were obtained from RiboBio Co. Ltd. (C10310-1; Guangzhou, China). Masson's trichrome stain kits (G1340) were from Solarbio Life Sciences (Beijing, China). Protein A/G PLUS-Agarose (#SC-223) was from Santa Cruz Biotechnology (Santa Cruz, CA, USA). The BCA Protein Assay Kit was obtained from CWBiotech (CW0014S; Beijing, China). All other chemicals used in this study were analytical grade and were made in China.

Table 1
Sequences of siRNAs that successfully suppressed target gene expression.

Name	Sequence
siRhoGDI1	Sense: 5′- CUUUCCGGGUUAACCGAGAdTdT-3′ Antisense: 5′- UCUCGGUUAACCCGGAAAGdTdT-3′
siRhoGDI2	Sense: 5′-CACAAGAGAACAAGAAUAAdTdT-3′ Antisense: 5′-UUAUUCUUGUUCUCUUGUGdTdT-3′

Table 2
Sequences of primers used in real-time RT-PCR.

Name	Sequence
RhoGDI1	F: 5′-ATCCAGGAGGCTGGGTATTG-3′ R: 5′-GCACGGACGGAGGCAATAAAT-3′
RhoGDI2	F: 5′-TTTATGGTTGGCAGCTATG-3′ R: 5′-GAGGTAGGTCTTGCTTGTC-3′
GAPDH	F: 5′-ACAACTCTCTCAAGATTGTCAGCAA -3′ R: 5′-ACTTTGTGAAGCTCATTTCCTGG-3′

2.2. Cell culture and treatment

Human aortic vascular smooth muscle cells (HA-VSMCs) were purchased from American Type Culture Collection (ATCC number: CRL-1999; Manassas, VA, USA). The cells were cultured in Ham's F12 K medium containing 2 mM L-glutamine supplemented with 10% FBS at 37 °C in a humidified 5% CO_2 incubator. Cells were used at passages 3–7. HA-VSMCs were exposed to Ang II (100 nM) at different time points (0, 6, 12, 24, and 48 h) or treated for 24 h with different concentrations of Ang II (0, 10, 100, and 1000 nM). In addition, where indicated, prior to Ang II treatment (100 nM), the cells were pretreated with candesartan (5 μM) or PD123319 (5 μM) for 6 h; MG132 (5 μM) for 1 h; PYR-41 (50 μM) for 30 min; ginkgolic acid (100 μM) for 4 h.

2.3. Cell proliferation assessment

Cell proliferation was measured using Cell-Light™ EdU Apollo®567

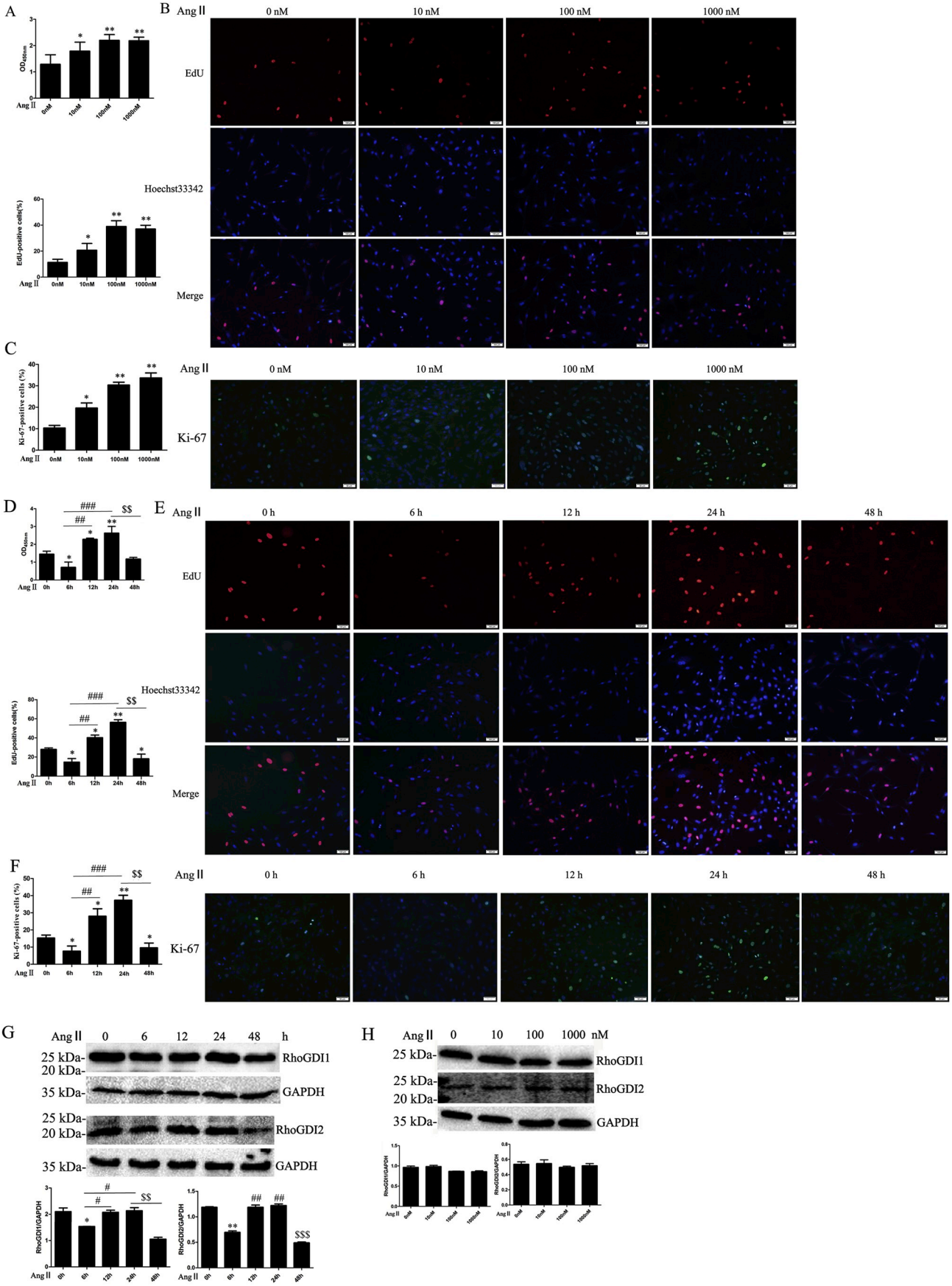

(caption on next page)

Fig. 1. The effects of Ang II on cell proliferation and the expression of RhoGDI1 and RhoGDI2 proteins in HA-VSMCs.
Cells were treated with Ang II at different concentrations (0, 10, 100, 1000 nM) or different time points (0, 6, 12, 24, 48 h). Untreated cells were used as the control group. (A and D) Cell proliferation was detected by BrdU assay after Ang II treatment. Histograms show the absorbance of each group at 450 nm. $*p < 0.05$ and $**p < 0.01$ *vs.* the control group. $\#\#p < 0.01$ and $\#\#\#p < 0.001$ *vs.* the group treated with Ang II for 6 h. $\$\$p < 0.01$ *vs.* the group treated with Ang II for 24 h (n = 5). (B and E) Cell proliferation was detected by EdU assay. Immunofluorescence shows EdU-positive cells (red). Nuclei were stained with Hoechst33342 (blue). Histograms show the ratios of EdU-positive cells to total cells. $*p < 0.05$ and $**p < 0.01$ *vs.* the control group; $\#\#p < 0.01$ and $\#\#\#p < 0.001$ *vs.* the group treated with Ang II for 6 h; $\$\$p < 0.01$ *vs.* the group treated with Ang II for 24 h (n = 5). (C and F) Immunofluorescence analysis of ki-67 expression (green). Nuclei were stained with DAPI (blue). Histograms show the ratios of ki-67-positive cells to total cells. $*p < 0.05$ and $**p < 0.01$ *vs.* the control group; $\#\#p < 0.01$ and $\#\#\#p < 0.001$ *vs.* the group treated with Ang II for 6 h; $\$\$p < 0.01$ *vs.* the group treated with Ang II for 24 h (n = 5). (G and H) Western blot analysis of RhoGDI1 (28 kDa) and RhoGDI2 (23 kDa) protein levels over a time course of treatment with 100 nM Ang II (G) and a range of doses of Ang II at 24 h (H). Histograms show the ratios of RhoGDI1 or RhoGDI2 to GAPDH. $*p < 0.05$ and $**p < 0.01$ *vs.* the control group; $\#p < 0.05$ and $\#\#p < 0.01$ *vs.* the group treated with Ang II for 6 h; $^{\$\$}p < 0.01$ and $^{\$\$\$}p < 0.001$ *vs.* the group treated with Ang II for 24 h (n = 5). (For interpretation of the references to colour in this figure legend, the reader is referred to the Web version of this article.)

In Vitro Imaging (100T) and Bromodeoxyuridine (BrdU) Proliferation Assay kits according to the manufacturer's instructions. After the treatments in 96-well plates, cells were labeled with EdU for 2 h or BrdU for 4 h. Cells labeled with EdU were fixed in 4% paraformaldehyde for 30 min and then permeabilized in 0.5% Triton X-100 for 10 min. Subsequently, cells were stained with Apollo and Hoechst33342 in the dark, and then washed and imaged using fluorescence microscopy (Nikon, Japan). Cells labeled with BrdU were incubated with anti-BrdU-peroxidase. Then, trimethyl benzidine substrate was added to the wells to detect the immune complex and the plates were measured at 450 nm using an ELISA plate reader (BioTek Instruments, Vermont, USA). The experiments were repeated three times, each using duplicate wells.

2.4. Western blotting

Cells were harvested and incubated with 40–50 μL Lysis buffer (1% NP-40, 1 mM PMSF) for 40 min. Then, the lysates were centrifuged at 4 °C for 15 min at 12,000 r/min, and the protein concentrations were determined using Bradford assays. The protein samples were separated using 12% SDS-polyacrylamide gel electrophoresis (PAGE) and transferred to nitrocellulose membranes (Merck Millipore Ltd. Ireland). The membranes were then blocked with 5% fat-free milk for 2 h at room temperature and incubated with primary antibodies overnight at 4 °C. The blots were detected by incubation with HRP-conjugated secondary antibodies for 2 h at room temperature followed by analysis with an ECL detection system (Amersham Biosciences). GAPDH was used as an internal standard. The relative intensities of the signals were quantified using densitometry and Imaging software (Labworks).

2.5. Co-immunoprecipitation

Cells were lysed in RIPA lysis buffer [50 mM Tris (pH 7.4), 150 mM NaCl, 1% Triton X-100, 1% sodium deoxycholate, 0.1% SDS] containing 1 mM PMSF and 25 mM NEM. After incubation on the ice for 20 min and centrifugation at 4 °C for 10 min at 12,000 r/min, the protein concentrations were determined using a BCA Protein Assay Kit. The lysates were incubated with specific antibodies (1:100) overnight at 4 °C, and then with Protein A/G PLUS-Agarose at room temperature for 2 h. Subsequently, the mixture was washed once with normal washing buffer (pH 7.4, 50 mM Tris-base, 100 mM NaCl, 1 mM Na_2-EDTA, 0.5% NP-40 containing 25 mM NEM) and five times with high salt washing buffer (pH 7.4, 50 mM Trise-base, 500 mM NaCl, 1 mM Na_2-EDTA, 0.5% NP-40 added containing 25 mM NEM). Pulled down proteins were boiled at 95 °C for 5 min in SDS loading buffer and analyzed by western blotting.

2.6. Real-time RT-PCR

Total RNA was extracted from HA-VSMCs using Total RNA Purification Kit in accordance with the manufacturer's instructions. One microgram of total RNA was reverse transcribed using a First Strand cDNA Synthesis Kit. The resulting cDNA was then mixed with Maxima SYBR Green qPCR Master Mix (Fermentas, Burlington, Canada) and specific primers (Table 2). The amplification conditions used for PCR cycling were as follows: 94 °C for 30 s, 57 °C for 30 s, and 72 °C for 30 s (RhoGDI1); 94 °C for 30 s, 54 °C for 30 s, and 72 °C for 30 s (RhoGDI2); 94 °C for 30 s, 54 °C for 30 s, and 72 °C for 30 s (GAPDH). Quantitative PCR was performed using a Corbett RG-6000 real-time PCR system (Corbett Life Sciences, Mortlake, Australia) according to the manufacturer's guidelines. The relative expression is shown after normalization to GAPDH.

2.7. siRNA transfection

Cells were transfected using Lipofectamine 2000 (#11668019; Invitrogen) according to the manufacturer's instruction. Briefly, the Lipofectamine 2000 transfection reagent and siRNAs (20 μM in DEPC water) were diluted with Opti-MEM (Invitrogen, Karlsruhe, Germany) and incubated at room temperature for 20 min. The mixture was then added to the cells and incubated for 48 h. Successful interference of the target gene was confirmed by western blotting. Subsequently, cells transfected with siRNAs were treated with 100 nM Ang II for 6, 12, 24, and 48 h.

2.8. Animals and Ang II infusion

Animal procedures were performed in accordance with the Ethics Committee and the Animal Care and Use Committee of Nantong University and conformed to the NIH Guide for the Care and Use of Laboratory Animals. Male C57Bl/6 mice aged 42–48 days weighing 20 ± 1 g were purchased from Beijing Vital River Laboratory Animal Technology Co., Ltd. (Beijing, China). Animals were randomly assigned into the following 5 groups (n = 8/group): control group (normal saline), model (Ang II infusion) group, Ad-RhoGDI1-shRNA treated group, Ad-RhoGDI2-shRNA treated group, Irbesartan treated group. The Adenoviral vectors specific for RhoGDI1 and RhoGDI2 shRNA were purchased from Hanheng Biotechnology (Shanghai, China). RhoGDI1-shRNA:GCAAGATTGACAAGACTGACTATTCAAGAGATAGTCAGTCTTGTCAATCTTGTTTTTT. RhoGDI2-shRNA:GAAACCATTGTGTTAAAGGAATTCAAGAGATTCCTTTAACACAATGGTTTCTTTTTT. Mice were anesthetized by intraperitoneal injection of 3.6% chloral hydrate (11 ml/kg). The right common carotid artery segment (4 cm) was isolated with two small atraumatic clips and injected with approximately 0.1 mL virus solution (titer of 1×10^{10} pfu) using a small needle. After incubation for 20 min, the clips were removed and the cervical wound was sutured. Irbesartan (50 mg/kg/d) was added to drinking water for consumption by mice. For Ang II infusion, mice were implanted with an Alzet Model 1002 osmotic minipump (Alzet Corp) for subcutaneous infusion of Ang II at a rate of 1000 ng/kg/min [30]. Control mice were implanted with pumps for infusion of normal saline. Pumps were placed into the subcutaneous space of anesthetized mice through a small incision in the back of the neck. The incision was closed and the mice were allowed to recover without medication. Mice were then

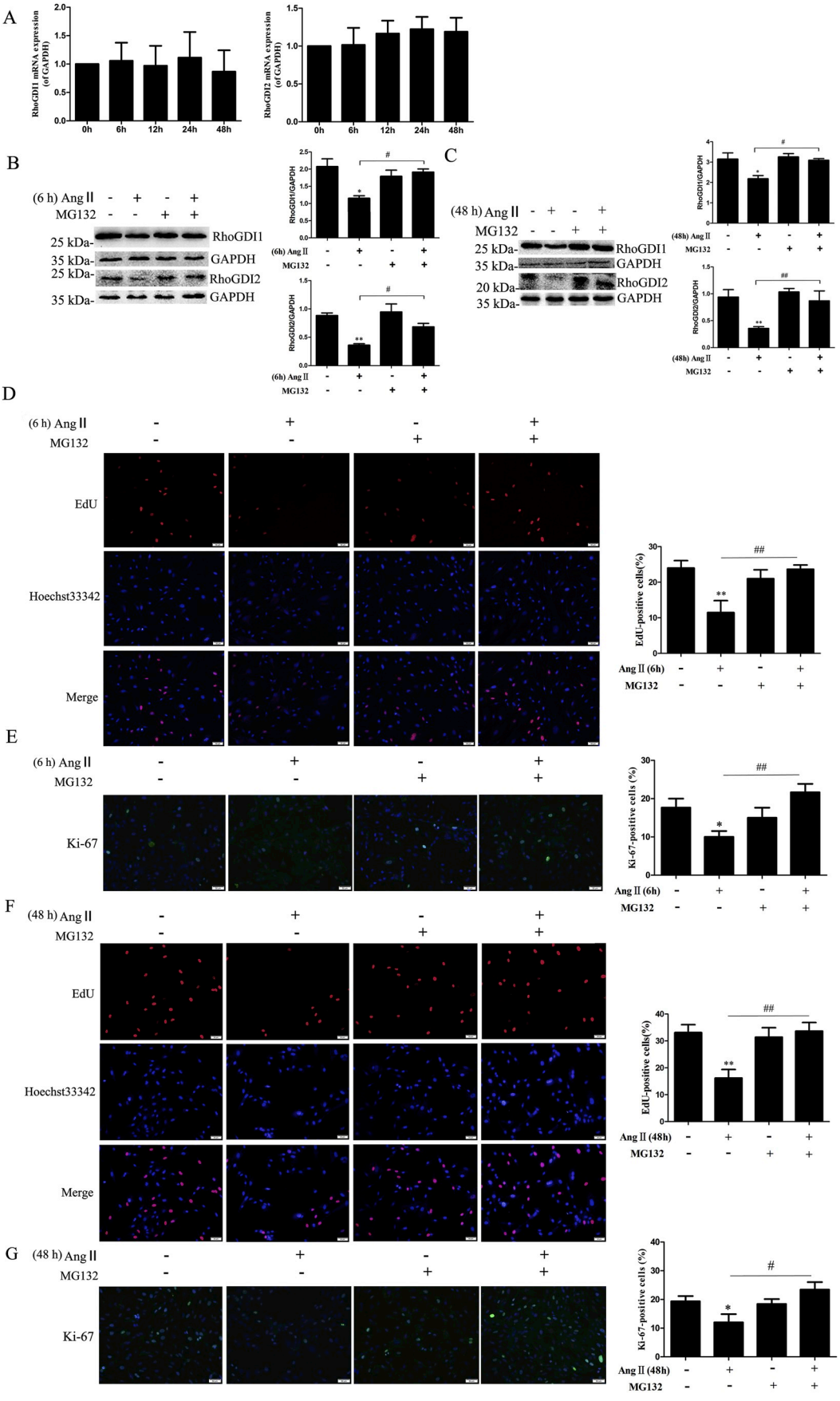

(caption on next page)

Fig. 2. The reduction in levels of RhoGDI1 and RhoGDI2 protein after Ang II treatment is mediated by proteosomal degradation.
(A) Real-time RT-PCR analysis of RhoGDI1 and RhoGDI2 mRNA levels. HA-VSMCs were treated with Ang II at different time points (0, 6, 12, 24, 48 h). Histograms show the ratios of *RhoGDI1* or *RhoGDI2* mRNA levels to *GAPDH* mRNA levels (n = 5). (B and C) Western blot analysis of RhoGDI1 and RhoGDI2. Cells were pretreated with MG132 (5 μM) for 1 h followed by 100 nM Ang II treatment for 6 h (B) or 48 h (C). Untreated cells were used as the control group. Histograms show the ratios of RhoGDI1 or RhoGDI2 to GAPDH. $*p < 0.05$ and $**p < 0.01$ *vs.* the control group; $\#p < 0.05$ and $\#\#p < 0.01$ *vs.* the Ang II-treated group (n = 5). (D and F) EdU analysis of cell proliferation. Immunofluorescence shows EdU-positive cells (red). Nuclei were stained with Hoechst33342 (blue). Cells were pretreated with MG132 (5 μM) for 1 h followed by 100 nM Ang II treatment for 6 h (D) or 48 h (F). Untreated cells were used as the control group. Histograms show the ratios of EdU-positive cells to total cells. $**p < 0.01$ *vs.* the control group; $\#\#p < 0.01$ *vs.* the Ang II-treated group (n = 5). (E and G) Ki-67 immunofluorescence of cell proliferation. Cells were pretreated with MG132 (5 μM) for 1 h followed by 100 nM Ang II treatment for 6 h (E) or 48 h (G). Untreated cells were used as the control group. Histograms show the ratios of ki-67-positive cells to total cells. $*p < 0.05$ *vs.* the control group; $\#p < 0.05$ and $\#\#p < 0.01$ *vs.* the Ang II-treated group (n = 5). (For interpretation of the references to colour in this figure legend, the reader is referred to the Web version of this article.)

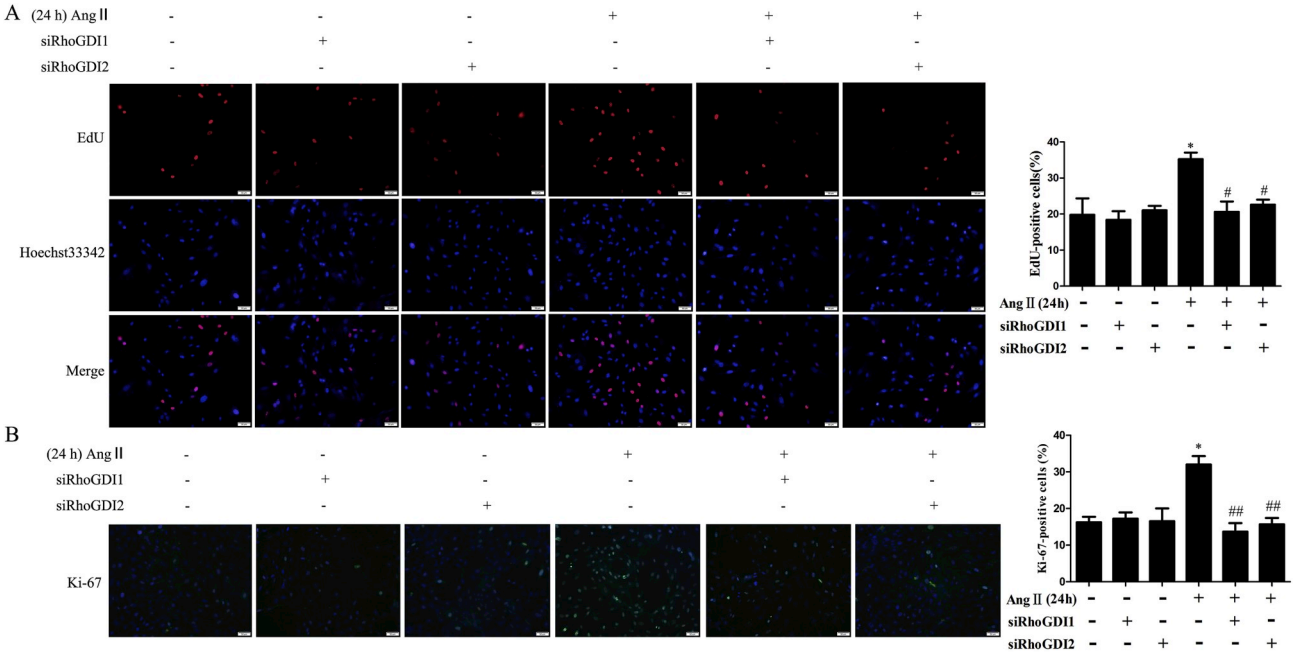

Fig. 3. Effects of RhoGDI1 or RhoGDI2 knockdown on Ang II-induced cell proliferation using EdU (A) and ki-67 assay (B).
Cells were treated with 100 nM Ang II for 24 h. Immunofluorescence shows EdU-positive cells (red) or ki-67-positive cells (green). Nuclei were stained with Hoechst33342 (blue) or DAPI (blue). Untreated cells belong to the control group. Histograms show the ratios of EdU-positive cells or ki-67-positive cells to total cells. $*p < 0.05$ *vs.* the control group; $\#p < 0.05$ and $\#\#p < 0.01$ *vs.* the Ang II-treated group (n = 5). (For interpretation of the references to colour in this figure legend, the reader is referred to the Web version of this article.)

euthanized at 14 days following Ang II infusion. The carotid arteries were removed and processed for subsequent analysis.

2.9. H&E staining and Masson's trichrome staining

Segments of the right common carotid arteries were isolated and fixed in 4% paraformaldehyde and then embedded in OCT (optimal cutting temperature compound). The embedded surface was trimmed with a cryo-microtome and then cryo-sectioned at a thickness of 5-μm. The sections were stained with hematoxylin aqueous solution for 5 min, hydrochloric acid for 30 s, and eosin for 2 min. The sections were then dehydrated using ethanol and cleared using xylene. For Masson's trichrome staining, the OCT-embedded sections were incubated overnight at room temperature in Bouin's fixative and stained with a Masson's Trichrome Kit. Nuclei were stained with Weigert's hematoxylin, myofiber cytoplasms were stained with Scarlet Red, and collagen was stained with Aniline Blue dye. All images were captured using an Olympus digital camera (Olympus, Tokyo, Japan) and analyzed using Image-Pro Plus software (Media Cybernetics, Rockville, MD, USA).

2.10. Immunofluorescence

Sections that were fixed with 4% paraformaldehyde were quenched with 5% BSA blocking buffer at 37 °C for 30 min and then incubated with primary antibodies (1:100 dilution in PBS) at 4 °C overnight. After three washes with PBS, the sections were incubated with biotin-conjugated anti-rabbit IgG for an additional 30 min at 37 °C. The sections were then stained with DAPI for 20 min and visualized with a fluorescence microscope using DyLight 488-SABC as a chromogen. The fluorescence intensity was quantified using ImagePro Plus software.

Sections were fixed with 4% paraformaldehyde for 20min, and then permeabilized in 0.5% Triton X-100 for 10min. Subsequently, the sections were incubated with ki-67 antibody (1:500) overnight at 4 °C and then with FITC-conjugated anti-rabbit IgG for 2 h at room temperature. Ki-67 positive cells were examined under a fluorescence microscope.

2.11. Statistical analysis

All results are expressed as means ± SDs. One-way ANOVA followed by Tukey's post-hoc tests were used for statistical analysis employing SPSS 22.0 software. A value of $p < 0.05$ was considered statistically significant.

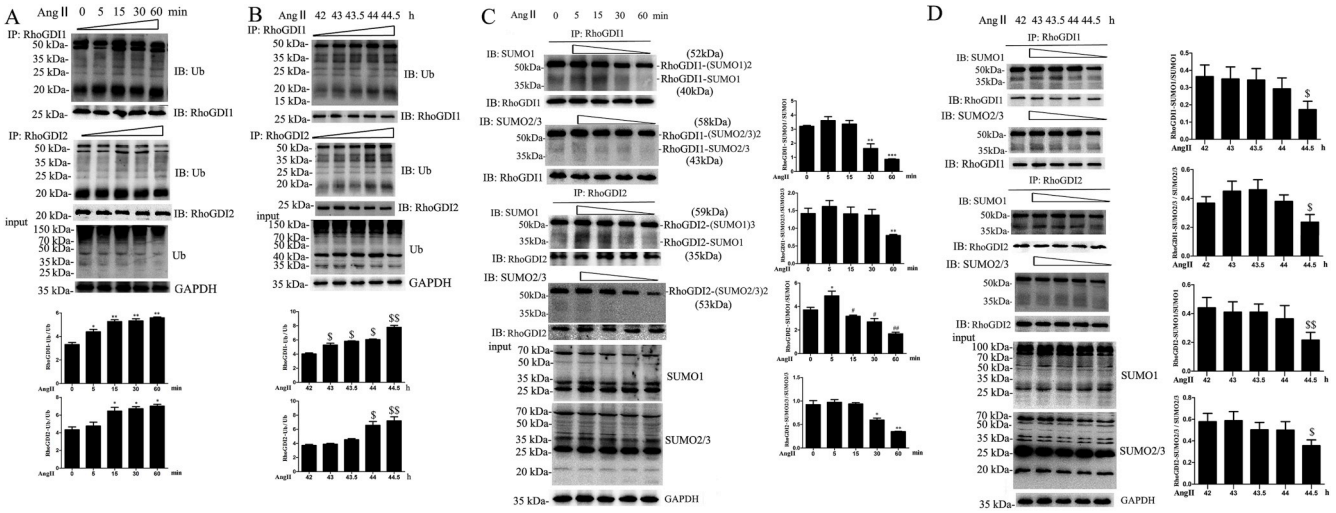

Fig. 4. Effects of Ang II on ubiquitination and SUMOylation of RhoGDI1 and RhoGDI2.
(A and B) Co-IP analysis of RhoGDI1 and RhoGDI2 ubiquitination. Cells were treated with Ang II (100 nM) for 0, 5, 15, 30, 60 min (A) or for 42, 43, 43.5, 44, 44.5 h (B). RhoGDI1 or RhoGDI2 was immunoprecipitated from cell lysates using specific antibodies, and then immunoprecipitated proteins were analyzed by Western blotting. Untreated cells were used as the control group. Histograms show the ratios of RhoGDI1-binding ubiquitin or RhoGDI2-binding ubiquitin to total ubiquitin. $^{*}p < 0.05$ and $^{**}p < 0.01$ *vs.* the control group (n = 5). $^{\$}p < 0.05$ and $^{\$\$}p < 0.01$ *vs.* the group treated with Ang II for 42 h (n = 5). (C and D) Co-IP analysis of RhoGDI1 and RhoGDI2 SUMOylation. Cells were treated with Ang II (100 nM) for 0, 5, 15, 30, 60 min, or for 42, 43, 43.5, 44, 44.5 h RhoGDI1 (28 kDa) or RhoGDI2 (23 kDa) was immunoprecipitated from cell lysates, and then immunoprecipitated proteins were analyzed by Western blotting with SUMO1 (12 kDa) and SUMO2/3 (15 kDa) antibodies. Histograms show the ratios of RhoGDI1-binding SUMO or RhoGDI2-binding SUMO to total SUMO. Untreated cells were used as the control group. $^{*}p < 0.05$, $^{**}p < 0.01$ and $^{***}p < 0.001$ *vs.* the control group; $\#p < 0.05$ and $\#\#p < 0.01$ *vs.* the group treated with Ang II for 5 min; \$, $p < 0.05$ and $^{\$\$}p < 0.01$ *vs.* the group treated with Ang II for 42 h (n = 5).

3. Results

3.1. RhoGDI stability participates in Ang II-mediated cell proliferation in HA-VSMCs

Ang II has crucial roles in the pathogenesis of vascular remodeling [8,31]. A growing body of evidence indicates that Ang II activates VSMC proliferation and migration in animal cells [7,32–34]. To investigate the effects of Ang II on phenotypic modulation in HA-VSMCs, we measured cell proliferation using BrdU, EdU assays, and ki-67 immunofluorescence staining after treatment with Ang II at different concentrations and time points. As shown in Fig. 1A–C, Ang II treatment for 24 h stimulated cell proliferation in a concentration-dependent manner in HA-VSMCs. However, 100 nM Ang II treatment exerted different effects on cell proliferation in HA-VSMCs at different time points (Fig. 1D–F). HA-VSMC proliferation decreased at 6 h of treatment with Ang II, followed by significant increases of cell proliferation at 12 and 24 h of treatment. Cell proliferation decreased again at 48 h of treatment with Ang II when compared with the proliferation at 0 h or 24 h. These results suggest that the effects of Ang II on HA-VSMC proliferation are both dose- and time-dependent.

To assess whether RhoGDI participates in the regulation by Ang II of HA-VSMC proliferation, we analyzed expression of RhoGDI1 and RhoGDI2 by Western blotting. Interestingly, the pattern of expression of RhoGDI1 and RhoGDI2, like the pattern of Ang II-mediated proliferation, was time-dependent. The protein levels of both RhoGDI1 and RhoGDI2 were reduced at 6 and 48 h of treatment with 100 nM Ang II (Fig. 1G). In addition, when compared with that of the 6 h Ang II treatment group, RhoGDI1 and RhoGDI2 protein levels at 12 and 24 h were significantly increased. However, in contrast with the pattern of Ang II-mediated proliferation, the protein levels of RhoGDI1 and RhoGDI2 at 12 and 24 h of Ang II treatment were not elevated above the level of untreated cells. Furthermore, the RhoGDI levels at 24 h of treatment with Ang II were not dose-dependent (Fig. 1H). These results suggest that the decreased levels of RhoRDI1 and RhoGDI2 at 6 and 48 h correlate with reduced proliferation, but that the increased proliferation at 12 and 24 h may be regulated by an alternate mechanism.

To determine whether the regulation of RhoGDI protein levels occurs at the level of mRNA expression, we performed real-time RT-PCR analysis. As shown in Fig. 2A, Ang II treatment did not affect the transcription levels of either RhoGDI1 or RhoGDI2. These results raise the possibility that RhoGDI protein may be subject to proteosomal degradation at 6 and 48 h of Ang II treatment. Therefore, we subsequently investigated the effects of the proteasome inhibitor MG132 on RhoGDI protein levels and cell proliferation in HA-VSMCs. As shown in Fig. 2B and C, RhoGDI1 and RhoGDI2 protein degradation induced by 6 and 48 h treatment of Ang II, was blocked by pretreatment with MG132. In contrast, at 12 and 24 h of Ang II treatment, MG132 pretreatment did not affect the expression of RhoGDI1 or RhoGDI2 and cell proliferation (Supplementary Fig. 1). Furthermore, MG132 pretreatment enhanced the proliferation of cells incubated with Ang II for 6 or 48 h (Fig. 2D–G), suggesting that the reduced proliferation of HA-VSMCs at 6 and 48 h Ang treatment may be regulated by proteosomal degradation of RhoGDIs.

To directly determine whether reduced RhoGDI protein levels affect HA-VSMC proliferation, we used siRNA to suppress the expression of RhoGDI1 and RhoGDI2 (Supplementary Fig. 2A). Reduced expression of either RhoGDI1 or RhoGDI2 caused a significant decrease in cell proliferation in HA-VSMCs treated with Ang II for 12 h (Supplementary Fig. 2B and C) and 24 h (Fig. 3). However, RhoGDI suppression exerted no obvious effect on the reduction of cell proliferation induced by 6 or 48 h of Ang II treatment (Supplementary Figs. 2B and C), when levels of RhoGDI are already reduced (Fig. 1G). These results are consistent with a role for RhoGDI proteosomal degradation in mediating the reduction in Ang II-dependent proliferation at 6 and 48 h.

3.2. Ang II regulates the stability of RhoGDI1 and RhoGDI2 through SUMOylation and ubiquitination via the AT1 receptor

Ubiquitination is the most important post-translational modification for protein degradation and plays a critical role in disease pathogenesis

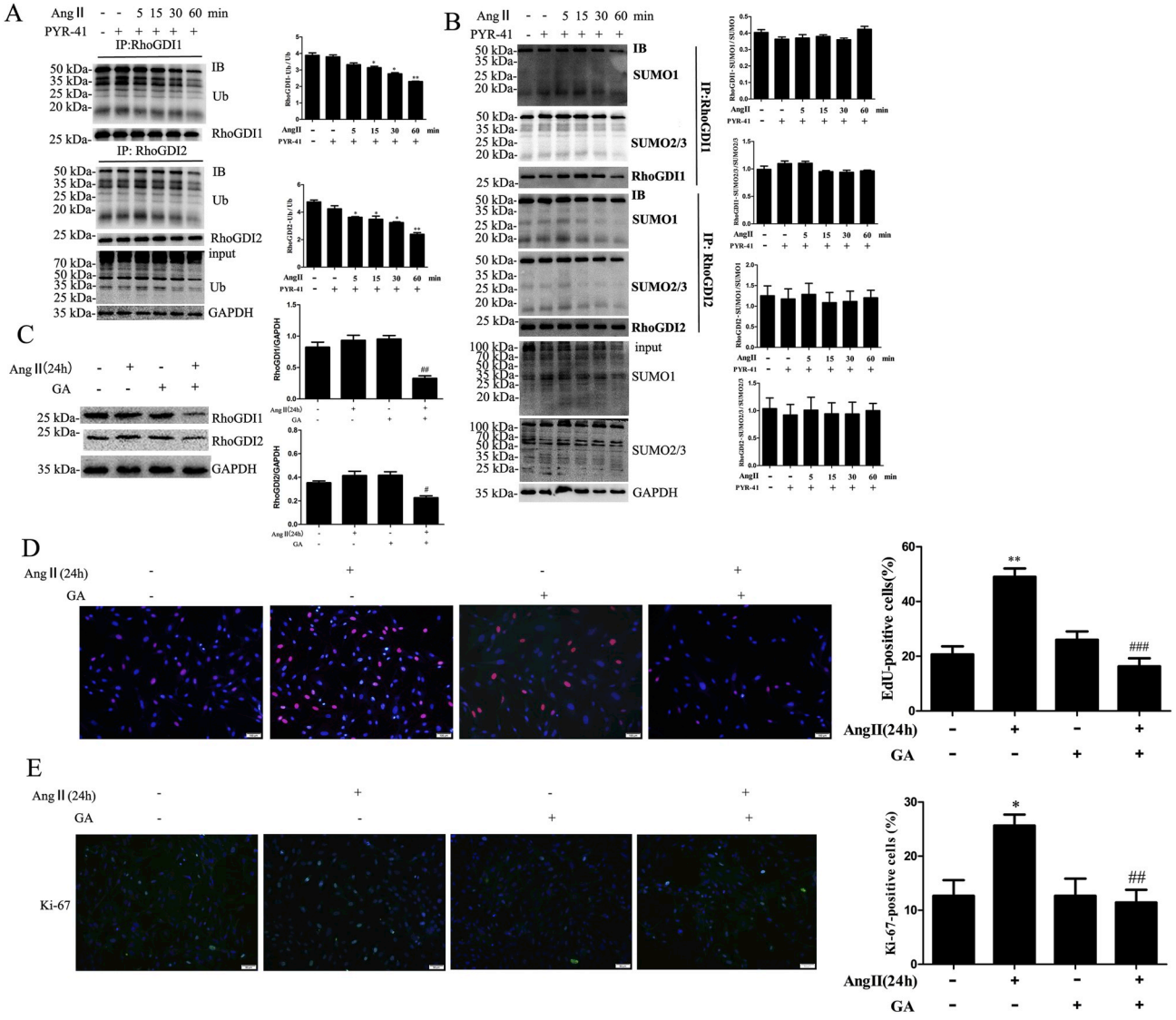

Fig. 5. SUMOylation stabilizes RhoGDI1 and RhoGDI2 proteins by competition with ubiquitination.
(A) Ubiquitination inhibitor PYR-41 decreased Ang II-induced RhoGDI1 and RhoGDI2 ubiquitination. Cells were pretreated with PYR-41 (50 μM) for 30 min and then stimulated with Ang II (100 nM) for 0, 5, 15, 30, 60 min RhoGDI1 or RhoGDI2 was immunoprecipitated from cell lysates, and then immunoprecipitated proteins were analyzed using Western blotting. Untreated cells were used as the control group. Histograms show the ratios of RhoGDI1-binding ubiquitin or RhoGDI2-binding ubiquitin to total ubiquitin. $*p < 0.05$ and $**p < 0.01$ *vs.* the control group (n = 5). (B) PYR-41 pretreatment inhibited the reduction in RhoGDI1 and RhoGDI2 SUMOylation induced by Ang II. Cells were pretreated with PYR-41 (50 μM) for 30 min and then stimulated with Ang II (100 nM) for 0, 5, 15, 30, 60 min RhoGDI1 or RhoGDI2 was immunoprecipitated from cell lysates, and then immunoprecipitated proteins were analyzed by western blotting with SUMO1 and SUMO2/3 antibodies. Histograms show the ratios of RhoGDI1-binding SUMO or RhoGDI2-binding SUMO to total SUMO (n = 5). (C) The SUMOylation inhibitor ginkgolic acid (GA) promoted RhoGDI1 and RhoGDI2 degradation. Cells were treated with 100 μM GA for 4 h, and then exposed to 100 nM Ang II for 24 h. Histograms show the ratios of RhoGDI1 or RhoGDI2 to GAPDH. $\#p < 0.05$ and $\#\#p < 0.01$ *vs.* the group treated with Ang II for 24 h (n = 5). (D and E) The effects of GA treatment on Ang II-induced cell proliferation were assessed by EdU and ki-67 assay. Untreated cells were used as the control group. Histograms show the ratios of EdU-positive cells or ki-67-positive cells to total cells. *, $p < 0.05$ and $**p < 0.01$ *vs.* the control group; $\#\#p < 0.01$ and $\#\#\#p < 0.001$ *vs.* the Ang II (24 h)-treated group (n = 5).

[35]. To clarify whether Ang II-induced RhoGDI protein degradation at 6 and 48 h of treatment is regulated by ubiquitin modification, we analyzed the ubiquitination levels of RhoGDI using Co-IP analysis. As demonstrated in Fig. 4A and B, the ubiquitin levels of both RhoGDI1 and RhoGDI2 were significantly increased between 0 and 60 min and 42–44.5 h of Ang II treatment, suggesting that Ang II (6 or 48 h) may stimulate RhoGDI protein degradation by up-regulating ubiquitination of RhoGDI. We also observed the ubiquitination of RhoGDI over a range of timepoints from 1 to 48 h of Ang II treatment. The ubiquitin levels of RhoGDI1 or RhoGDI2 were gradually decreased after 1 h Ang II treatment, and began to increase after 43 h of Ang II treatment (Supplementary Fig. 3A), indicating that the stable RhoGDI protein levels at 12 or 24 h of Ang II treatment are associated with decreased levels of RhoGDI ubiquitination.

It has been reported that SUMOylation and ubiquitination reciprocally regulate α-synuclein degradation and pathological aggregation in Parkinson's disease (PD) [27]. Therefore, we assessed SUMOylation of RhoGDI after Ang II treatment between 0 and 48 h. As shown in Fig. 4C and D, RhoGDI1 was modified by one or two SUMO1 or one or two SUMO2/3 molecules, and RhoGDI2 was modified by one or three SUMO1 or two SUMO2/3 molecules. SUMO1-modified RhoGDI2 showed a transient increase after 5 min treatment of Ang II, followed by a significant decrease after 15 min of Ang II treatment. Ang II treatment for 60 min also significantly reduced the levels of SUMO1- and SUMO2/

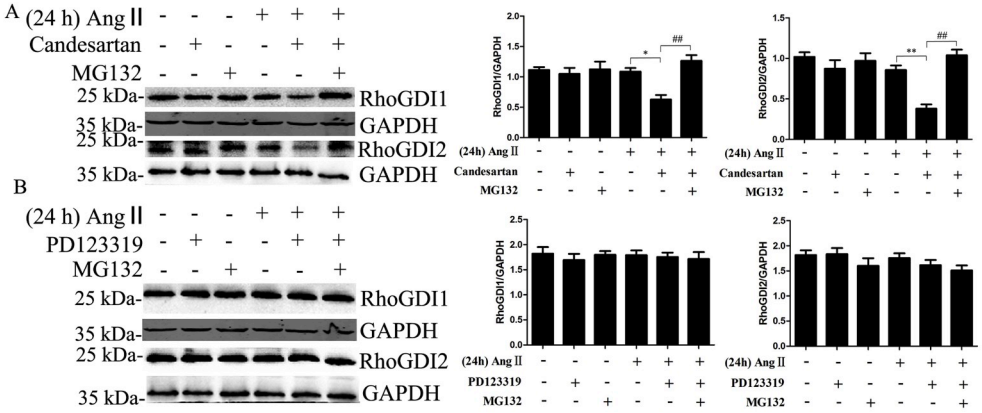

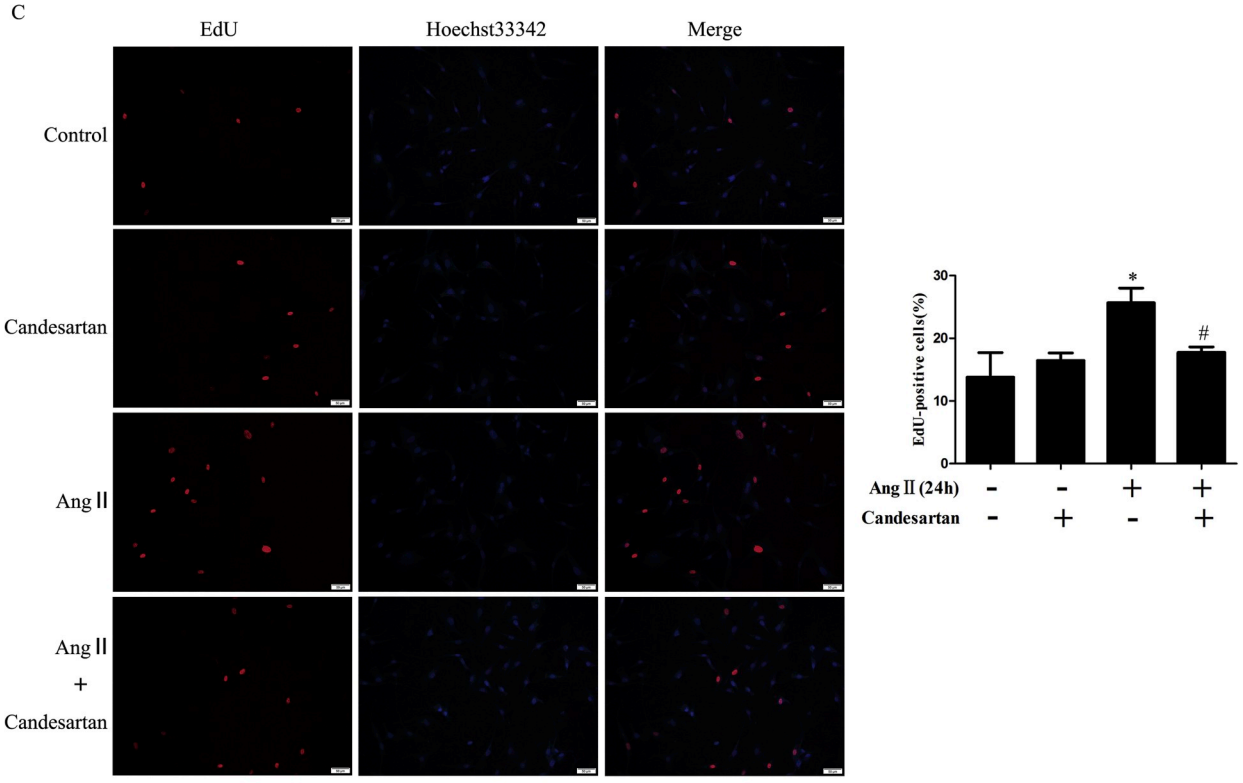

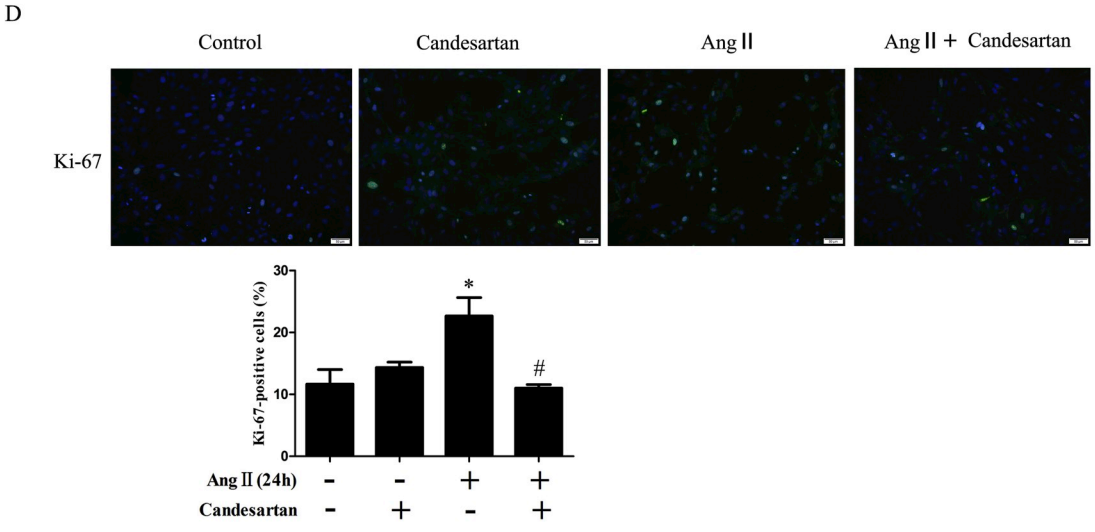

(caption on next page)

Fig. 6. The effects of Ang II receptor inhibitors on RhoGDI1 and RhoGDI2 protein levels and cell proliferation.
(A) The AT1 receptor inhibitor candesartan induced RhoGDI1 and RhoGDI2 protein degradation. Cells were pretreated with candesartan (5 μM) for 6 h or MG132 (5 μM) for 1 h and then exposed to 100 nM Ang II for 24 h. Cell lysates were analyzed by western blotting with RhoGDI1 and RhoGDI2 antibodies. Histograms show the ratios of RhoGDI1 or RhoGDI2 to GAPDH. $*p < 0.05$ and $**p < 0.01$ *vs.* the group treated with Ang II for 24 h; $\#\#p < 0.01$ *vs.* the group treated with candesartan and Ang II (n = 5). (B) The AT2 receptor inhibitor PD123319 exerted no significant effect on RhoGDI1 and RhoGDI2 protein levels. Cells were pretreated with PD123319 (5 μM) for 6 h or MG132 (5 μM) for 1 h and then exposed to 100 nM Ang II for 24 h. Cell lysates were analyzed by western blotting with RhoGDI1 and RhoGDI2 antibodies. Histograms show the ratios of RhoGDI1 or RhoGDI2 to GAPDH (n = 5). (C and D) Candesartan reduced Ang II-mediated cell proliferation in HA-VSMCs. Cell proliferation was detected by EdU assay and ki-67 immunofluorescence. Cells were pretreated with candesartan (5 μM) for 6 h and then exposed to 100 nM Ang II for 24 h. Histograms show the ratios of EdU-positive cells or ki-67-positive cells to total cells. Untreated cells were used as the control group. $*p < 0.05$ *vs.* the control group; $\#p < 0.01$ *vs.* the Ang II-treated group (n = 5).

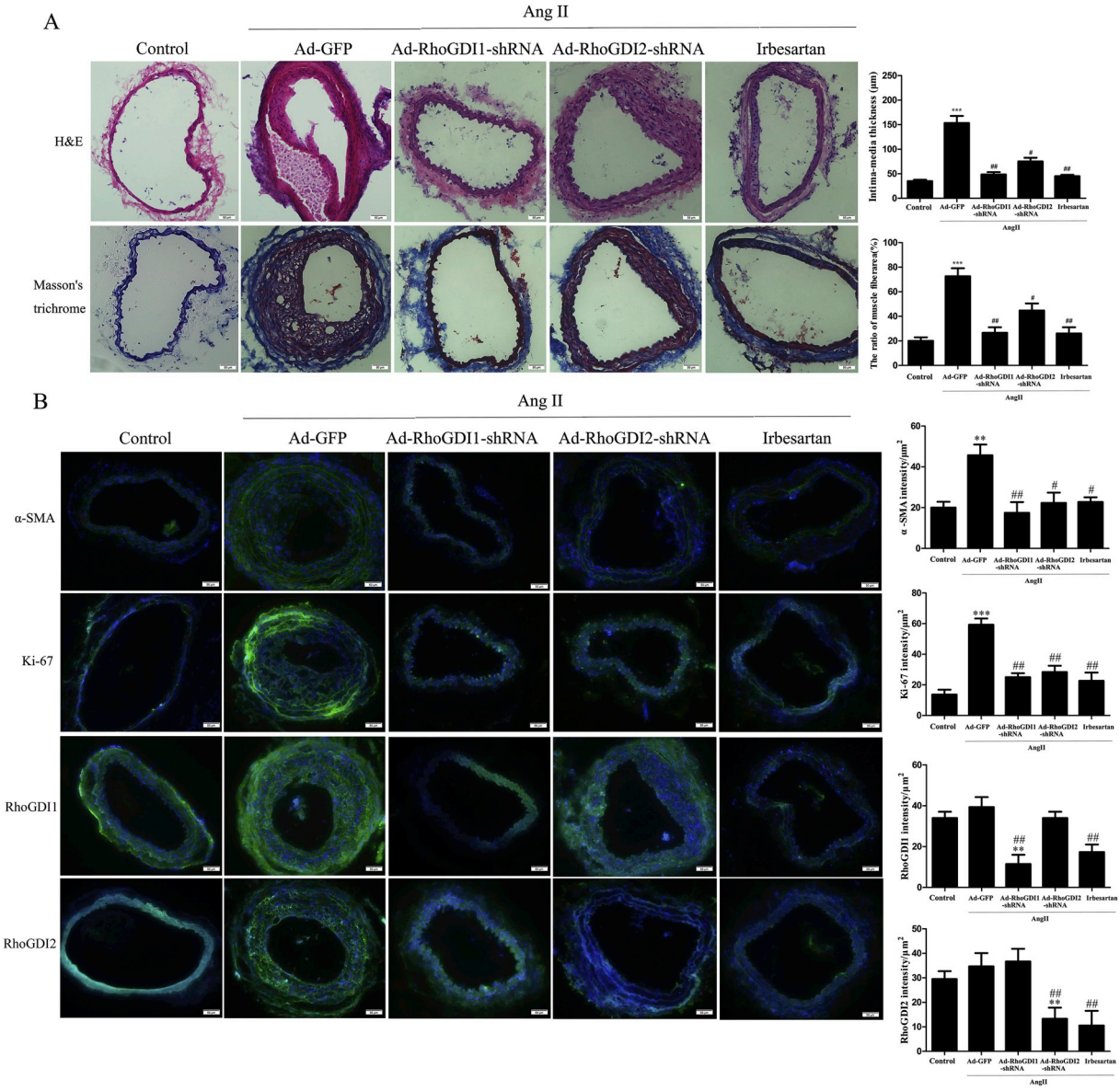

Fig. 7. The effects of RhoGDI suppression and Irbesartan on vascular remodeling and target protein expression in mice.
For shRNA-mediated knockdown, the right common carotid arteries of mice were injected and incubated with 1×10^{10} pfu virus solution for 20 min. The AT1 receptor inhibitor Irbesartan (50 mg/kg/d) was added to drinking water for consumption by mice. Ang II was subcutaneously infused at a rate of 1000 ng/kg/min using the Alzet Model 1002 osmotic minipump. (A) Representative photographs of H&E staining and Masson's trichrome staining of carotid arteries 14 days after Ang II infusion. Masson's trichrome staining shows the collagen fibers (blue) and muscle fibers (red). Mice with normal saline infusion were used as the control group. Histograms show the intima-media thickness (IMT) and the ratio of muscle fiber area. $***p < 0.001$ *vs.* the control group; $\#p < 0.05$ and $\#\#p < 0.01$ *vs.* the model group (Ang II infusion + Ad-GFP virus) (n = 8). (B) Immunofluorescence staining of α-SMA, Ki-67, RhoGDI1, and RhoGDI2 (green). Nuclei were stained with DAPI (blue). Histograms show the fluorescence intensity of the staining. $**p < 0.01$ and $***p < 0.001$ *vs.* the control group; $\#p < 0.05$ and $\#\#p < 0.01$ *vs.* the model group (Ang II infusion + Ad-GFP virus) (n = 8). (For interpretation of the references to colour in this figure legend, the reader is referred to the Web version of this article.)

3-modified RhoGDI1 and RhoGDI2 when compared with the untreated group (Fig. 4C), and Ang II treatment for 44.5 h significantly reduced levels of SUMO1- and SUMO2/3-modified RhoGDI1 and RhoGDI2 when compared with 42 h-treated group (Fig. 4D). Further analysis of the time points between the decreases in SUMOylation showed that levels of SUMOylated RhoGDI1 and RhoGDI2 gradually increased after 1 h treatment of Ang II until 43 h and then decreased after 48 h of treatment (Supplementary Fig. 3B). Therefore, the SUMOylation of RhoGDI in response to Ang II is reciprocal to its ubiquitination and correlates with time points during which protein levels are restored to basal levels.

To evaluate whether RhoGDI ubiquitination may influence RhoGDI SUMOylation, we assessed the effects of the UBE1 (ubiquitin-activating enzyme E1) inhibitor PYR-41 on RhoGDI SUMOylation. PYR-41 treatment significantly inhibited the ubiquitination of RhoGDI after 60min (Fig. 5A) and 43–48 h (Supplementary Fig. 4A) of treatment with Ang II, as expected. Furthermore, the addition of PYR-41 led to increased levels of SUMOylation (Fig. 5B and Supplementary Fig. 4B), indicating that ubiquitin and SUMO proteins may compete for binding to RhoGDI. These data also raised the possibility that SUMOylation might facilitate RhoGDI stability by inhibiting ubiquitin-dependent protein degradation. To assess this possibility, we evaluated the effect of the SUMOylation inhibitor ginkgolic acid (GA) on RhoGDI protein levels and cell proliferation. As shown in Fig. 5C and Supplementary Fig. 5, GA pretreatment decreased the protein levels of RhoGDI1 and RhoGDI2 in HA-VSMCs treated with Ang II for 12 or 24 h, but did not affect the levels at 6 or 48 h of Ang II-treatment. GA pretreatment also significantly reduced cell proliferation induced by 12 or 24 h of Ang II-treatment with no significant effect on proliferation at 6 or 48 h (Fig. 5D and E and Supplementary Fig. 6).

To evaluate the role of Ang II receptors AT1 and AT2 on Ang II-dependent RhoGDI stability, we examined the effects of AT1 or AT2 receptor inhibitor on the protein levels of RhoGDI after Ang II treatment of HA-VSMCs. As shown in Fig. 6 and Supplementary Fig. 7, pretreatment with the AT1 receptor inhibitor candesartan obviously reduced RhoGDI1 and RhoGDI2 protein levels at 12 and 24 h, and these reductions were reversed by MG132 treatment. In contrast, pretreatment with the AT2 receptor inhibitor PD123319 did not significantly affect RhoGDI protein levels at 12 or 24 h treatment with Ang II. Furthermore, neither candesartan nor PD123319 prevented Ang II- dependent reduction in RhoGDI protein levels at 6 or 48 h, though these reduced levels were blocked by MG132 (Supplementary Fig. 7). These data suggest that signaling through AT1 receptor at 12 and 24 h stabilizes RhoGDI by reducing Ang II-dependent RhoGDI degradation.

To verify that AT1 receptor-mediated signaling promotes Ang II-induced cell proliferation in HA-VSMCs, we repeated EdU and ki-67 assays in the absence or presence of candesartan. As shown in Fig. 6C and D and Supplementary Fig. 8, the proportion of EdU-positive or ki-67-positive cells was significantly increased after 12 or 24 h Ang II treatment, while this increase was reversed by candesartan. In contrast, candesartan did not affect Ang II-induced reduction (6 or 48 h) of cell proliferation, which was instead blocked by MG132 (Supplementary Fig. 8). Taken together, these findings suggest that the AT1 receptor, but not AT2 receptor, mediates Ang II-dependent maintenance of RhoGDI stability at 12 or 24 h, which leads to cell proliferation in HA-VSMCs.

3.3. RhoGDI plays a key role in Ang II-mediated muscle cell proliferation and vascular remodeling in mice

We next verified the effects of RhoGDI suppression and AT1 receptor inhibition on vascular remodeling *in vivo* using a mouse Ang II infusion model. As shown in Fig. 7A, Ang II infusion resulted in significant vascular remodeling, as assessed by H & E staining and quantification of the intima-media thickness (IMT; 35.55 ± 2.21 vs. 158.67 ± 10.66 μm, $p < 0.001$). Knockdown of either RhoGDI1 or RhoGDI2 significantly reduced neointima formation, as evidenced by 69% and 52% decreases in the IMT. In addition, the AT1 receptor inhibitor Irbesartan reduced Ang II-mediated vascular remodeling, as evidenced by a 72% decrease in the IMT. To investigate whether RhoGDI and AT1 receptor participate in muscle fibrosis, we also examined collagen and myofiber production by Masson's trichrome staining. The density of trichrome blue staining (collagen) and the muscle fiber area (red staining) were significantly increased after Ang II infusion, and these effects were inhibited by RhoGDI knockdown or Irbesartan treatment (Fig. 7A). To verify the effects of Ang II and RhoGDI on the *in vivo* proliferation of VSMCs, we performed immunostaining assay for α-SMA and Ki-67. Knockdown of RhoGDI (either RhoGDI1 or RhoGDI2) and Irbesartan treatment reduced the expression of α-SMA and Ki-67 after Ang II infusion in mice (Fig. 7B), which confirms that the RhoGDIs and AT1 receptor are required for AngII-mediate proliferation of VSMCs. These results are consistent with our *in vitro* results with HA-VSMCs. Importantly, Ang II infusion did not significantly affect the expression of RhoGDI1 and RhoGDI2 (Fig. 7B). However, Irbesartan treatment reduced the protein levels of both RhoGDI1 and RhoGDI2, which is consistent with a role for AT1 receptor signaling in protecting cells from RhoGDI degradation. Overall, these results suggest that RhoGDI stability and AT1 receptor signaling participate in Ang II-induced myofiber deposition and vascular remodeling.

4. Discussion

Ang II has been implicated in various cardiovascular diseases including hypertension and atherosclerosis via multiple signal pathways, especially Rho signaling. It has been reported that the Rho/ROCK pathway plays an important role in Ang II-induced cardiac remodeling [36,37], vasoconstriction [38,39], endothelial progenitor cell function [40], and human Bartter's and Gitelman's Syndromes [41]. In addition, the RhoA pathway by Ang II is activated in VSMCs from SHRSP (stroke-prone spontaneously hypertensive) rats and is involved in rat VSMC remodeling [42,43]. RhoGDIs have been shown to negatively regulate Rho-family GTPases and to play important regulatory roles in many intracellular processes including cell adhesion, proliferation, migration, and tumorigenesis [10,11,14,15]. RhoGDI has also been reported to be involved in ERK activation in response to mechanical stress-induced hypertrophy, but not Ang II-induced ERK activation in rat cardiomyocytes [18,44]. RhoGDI also has been shown to participate in the Ang II-induced promoter activity of the skeletal α-actin and c-fos genes [18,19]. However, prior to this study, the roles of RhoGDIs in Ang II-induced smooth muscle phenotypic modulation and vascular remodeling remained uncharacterized. In this study, for the first time, we demonstrated that RhoGDI1 and RhoGDI2 stability, rather than protein expression, is regulated by SUMOylation and ubiquitination via AT1 receptor and participates in Ang II-induced HA-VSMC phenotypic modulation and vascular remodeling.

Many studies have reported that Ang II promotes cell proliferation in VSMCs [6,7]. However, in this study, we demonstrated that cell proliferation was first reduced at 6 h of Ang II treatment, and then was significantly increased until 24 h of Ang II treatment in HA-VSMCs. Furthermore, Ang II-induced proliferation was decreased again after 48 h of treatment. It has been reported that RhoGDI expression levels do not differ in SHRSP and WKY (Wistar-Kyoto) rats [42]. Another report showed that Ang II induces the upregulation of RhoGDIα via the AT1 receptor in spontaneously hypertensive rats [20]. Interestingly, in this study the protein levels of both RhoGDI1 and RhoGDI2 were decreased at 6 and 48 h and showed a similar trend as cell proliferation upon induction by Ang II in HA-VSMCs. These results may imply that Ang II exerts different regulatory effects on RhoGDI protein in rat cell lines and human cell lines. In addition, in this study we demonstrated that the protease inhibitor MG132 significantly inhibited the decreases in the RhoGDI protein level and cell proliferation rate induced by Ang II

treatment at 6 h and 48 h, although it had no significant effect on the RhoGDI protein level and cell proliferation following 12- or 24 h-Ang II-treatment cells. Furthermore, suppressing RhoGDI1 and RhoGDI2 significantly decreased Ang II–induced (12 or 24 h) HA-VSMC proliferation. These results suggest that RhoGDIs are involved in Ang II-induced HA-VSMC proliferation and are regulated at the level of stability, rather than expression.

Ubiquitin (Ub) is crucial for various pathophysiological processes, including cell survival and differentiation, and marks proteins for degradation [35]. Small ubiquitin-related modifier (SUMO) is an additional post-translational protein modifier that protects proteins from degradation [21,22]. In the current study, we demonstrated that the increased ubiquitination and decreased SUMOylation of RhoGDI1 and RhoGDI2 at 60 min, and 42–48 h of Ang II treatment caused the degradation of RhoGDI. In addition, ubiquitination inhibition (PYR-41) significantly prevented the decreased SUMOylation of RhoGDI1 and RhoGDI2, suggesting that Ub and SUMO competitively bind to RhoGDI1 and RhoGDI2. Therefore, we speculate that RhoGDI protein degradation induced by Ang II at 6 h and 48 h was mainly due to its higher ubiquitination versus SUMOylation. Importantly, SUMOylation inhibition (GA) significantly reduced RhoGDI1 and RhoGDI2 protein levels and cell proliferation induced by Ang II at 12 or 24 h, indicating that SUMOylation plays an important role in maintaining RhoGDI1 and RhoGDI2 stability and cell proliferation mediated by Ang II. Furthermore, AT1 receptor inhibition reduced RhoGDI1 and RhoGDI2 protein levels and cell proliferation induced by Ang II at 12 or 24 h, suggesting that the activation of the AT1 receptor, but not the AT2 receptor, participates in the preservation of RhoGDI stability and cell proliferation in HA-VSMCs. Moreover, the AT1 receptor inhibitor candesartan did not affect Ang II -induced reduction (6 or 48 h) of RhoGDI protein levels or cell proliferation. Our data suggest that RhoGDI stabilization by SUMOylation induced by Ang II at 12 and 24 h is dependent on the AT1 receptor, but that RhoGDI ubiquination and degradation and reduced cell proliferation induced by Ang II at 6 h and 48 h might be independent of the AT1 receptor.

We also demonstrated that RhoGDI1, RhoGDI2, and AT1 receptor participate in VSMC proliferation and vascular remodeling in mice after Ang II infusion; these effects were significantly inhibited by RhoGDI1 or RhoGDI2 knockdown and Irbesartan treatment. However, Ang II infusion did not significantly promote RhoGDI1 and RhoGDI2 protein levels when compared with the control group. This indicates that Ang II does not cause vascular remodeling by increasing RhoGDI protein levels or its expression, which is consistent with its function in stabilizing RhoGDI protein. Moreover, AT1 receptor inhibition dramatically decreased RhoGDI1 and RhoGDI2 protein levels in mice after Ang II infusion *in vivo*, suggesting that Irbesartan treatment inhibits vascular remodeling by, or at least in part by reducing RhoGDI protein levels. Consistent with the *in vitro* results, these findings suggest that Ang II stabilizes RhoGDI protein via the AT1 receptor, which plays a role in HA-VSMC proliferation and vascular remodeling. Further studies are necessary to better understand the mechanisms underlying the regulation by ubiquitination and SUMOylation of RhoGDI stability in Ang II-mediated vascular remodeling *in vivo*. It has been reported that RhoGDIα suppression decreases Ang II-induced superoxide production and lipid peroxidation, and inhibition of Ang II-induces leucine incorporation [5]. Therefore, RhoGDI may represent a target for anti-hypertrophic pharmacologic interventions. However, our results also raise the possibility that RhoGDI knockdown or its targeted degradation may provide a novel approach for treatment of vascular remodeling.

In summary, the main findings in this study are: (1) the stability of RhoGDI1 and RhoGDI2, but not their expression, participates in the regulation by Ang II of smooth muscle phenotypic transformation and vascular remodeling; (2) SUMOylation and ubiquitination reciprocally regulate RhoGDI stability via the AT1 receptor.

Conflicts of interest

The authors declared they do not have anything to disclose regarding conflict of interest with respect to this manuscript.

Financial support

This work was supported by a grant from the National Natures Science Foundation of Nantong City (No. JC2018059), the Jiangsu Planned Projects for Postdoctoral Research Funds (No. 1601107C), and the Postgraduate Research & Practice Innovation Program of Jiangsu Province (No. KYCX19_2085).

Appendix A. Supplementary data

Supplementary data to this article can be found online at https://doi.org/10.1016/j.atherosclerosis.2019.07.010.

References

[1] E.L. Schiffrin, Vascular remodeling in hypertension mechanisms and treatment, Hypertension 59 (2) (2012) 367–374.
[2] G.K. Owens, M.S. Kumar, B.R. Wamhoff, Molecular regulation of vascular smooth muscle cell differentiation in development and disease, Physiol. Rev. 84 (3) (2004) 767–801.
[3] A. Nguyen Dinh Cat, A.C. Montezano, D. Burger, R.M. Touyz, Angiotensin II, NADPH oxidase, and redox signaling in the vasculature, Antioxidants Redox Signal. 19 (10) (2013) 1110–1120.
[4] C.A. Lemarié, E.L. Schiffrin, The angiotensin II type 2 receptor in cardiovascular disease, J. Renin-Angiotensin-Aldosterone Syst. JRAAS 11 (1) (2010) 19–31.
[5] P.K. Mehta, K.K. Griendling, Angiotensin II cell signaling: physiological and pathological effects in the cardiovascular system, Am. J. Physiol. Cell Physiol. 292 (1) (2007) C82–C97.
[6] A. Rodríguez, J. Gómez-Ambrosi, V. Catalán, A. Fortuño, G. Frühbeck, Leptin inhibits the proliferation of vascular smooth muscle cells induced by angiotensin II through Nitric Oxide-dependent mechanisms, Mediat. Inflamm. 2010 (2010) 105489.
[7] J.F. Cheng, G.H. Ni, M.F. Chen, Y.J. Li, Y.J. Wang, C.L. Wang, Q. Yuan, R.Z. Shi, C.P. Hu, T.L. Yang, Involvement of profilin-1 in angiotensin II-induced vascular smooth muscle cell proliferation, Vasc. Pharmacol. 55 (1–3) (2011) 34–41.
[8] T. Takayanagi, T. Kawai, S.J. Forrester, T. Obama, T. Tsuji, Y. Fukuda, K.J. Elliott, D.G. Tilley, R.L. Davisson, J.Y. Park, S. Eguchi, Role of epidermal growth factor receptor and endoplasmic reticulum stress in vascular remodeling induced by angiotensin II, Hypertension 65 (6) (2015) 1349–1355.
[9] E. Boulter, R. Garcia-Mata, RhoGDI: a rheostat for the Rho switch, Small GTPases 1 (1) (2010) 65–68.
[10] E. Boulter, R. Garcia-Mata, C. Guilluy, A. Dubash, G. Rossi, P.J. Brennwald, K. Burridge, Regulation of RhoGTPase crosstalk, degradation and activity by RhoGDI1, Nat. Cell Biol. 12 (5) (2010) 477–483.
[11] R. Garcia-Mata, E. Boulter, K. Burridge, The 'invisible hand': regulation of RHO GTPases by RHOGDIs, Nat. Rev. Mol. Cell Biol. 12 (8) (2012) 493–504.
[12] N.K. Agarwal, D. Kazyken, D.D. Sarbassov, Rictor encounters RhoGDI2: the second pilot is taking a lead, Small GTPases 4 (2) (2013) 102–105.
[13] C. DerMardirossian, G.M. Bokoch, GDIs: central regulatory molecules in Rho GTPase activation, Trends Cell Biol. 15 (7) (2005) 356–363.
[14] M.B. Jones, H. Krutzsch, H. Shu, Y. Zhao, L.A. Liotta, E.C. Kohn, E.F. Petricoin, Proteomic analysis and identification of new biomarkers and therapeutic targets for invasive ovarian cancer, Proteomics 2 (1) (2002) 76–84.
[15] L. Zhao, H. Wang, X. Sun, Y. Ding, Comparative proteomic analysis identifies proteins associated with the development and progression of colorectal carcinoma, FEBS J. 277 (20) (2010) 4195–4204.
[16] M.A. Forget, R.R. Desrosiers, M. Del, R. Moumdjian, D. Shedid, F. Berthelet, R. Beliveau, The expression of rho proteins decreases with human brain tumor progression: potential tumor markers, Clin. Exp. Metastasis 19 (1) (2002) 9–15.
[17] M.A. Harding, D. Theodorescu, RhoGDI2: a new metastasis suppressor gene: discovery and clinical translation, Urol. Oncol. 25 (5) (2007) 401–406.
[18] R. Aikawa, I. Komuro, T. Yamazaki, Y. Zou, S. Kudoh, W. Zhu, T. Kadowaki, Y. Yazaki, Rho family small G proteins play critical roles in mechanical stress–induced hypertrophic responses in cardiac myocytes, Circ. Res. 84 (4) (1999) 458–466.
[19] R. Aikawa, I. Komuro, R. Nagai, Y. Yazaki, Rho plays an important role in angiotensin II induced hypertrophic responses in cardiac myocytes, Mol. Cell. Biochem. 212 (1–2) (2000) 177–182.
[20] Y.L. Bian, Y.X. Qi, Z.Q. Yan, D.K. Long, B.R. Shen, Z.L. Jiang, A proteomic analysis of aorta from spontaneously hypertensive rat: RhoGDI alpha upregulation by angiotensin II via AT1 receptor, Eur. J. Cell Biol. 87 (2) (2008) 101–110.
[21] A. Flotho, F. Melchior, Sumoylation: a regulatory protein modification in health and disease, Annu. Rev. Biochem. 82 (2013) 357–385.
[22] M.C. Geoffroy, R.T. Hay, An additional role for SUMO in ubiquitin-mediated proteolysis, Nat. Rev. Mol. Cell Biol. 10 (8) (2009) 564–568.

[23] K. Eifler, A.C. Vertegaal, SUMOylation-mediated regulation of cell cycle progression and cancer, Trends Biochem. Sci. 40 (12) (2015) 779–793.
[24] B. Guo, S.H. Yang, J. Witty, A.D. Sharrocks, Signalling pathways and the regulation of SUMO modification, Biochem. Soc. Trans. 35 (6) (2007) 1414–1418.
[25] Y. Zhang, Y.Y. Li, B. Tang, C.Y. Zhang, The strategies for identification and quantification of SUMOylation, Chem. Commun. 53 (52) (2017) 6989–6998.
[26] A. Pichler, C. Fatouros, H. Lee, N. Eisenhardt, SUMO conjugation-a mechanistic view, Biomol. Concepts 8 (1) (2017) 13–36.
[27] R. Rott, R. Szargel, V. Shani, H. Hamza, M. Savyon, F. Abd Elghani, R. Bandopadhyay, S. Engelender, SUMOylation and ubiquitination reciprocally regulate α-synuclein degradation and pathological aggregation, Proc. Natl. Acad. Sci. U.S.A. 114 (50) (2017) 13176–13181.
[28] H.B. Luo, Y.Y. Xia, X.J. Shu, Z.C. Liu, Y. Feng, X.H. Liu, G. Yu, G. Yin, Y.S. Xiong, K. Zeng, J. Jiang, K. Ye, X.C. Wang, J.Z. Wang, SUMOylation at K340 inhibits tau degradation through deregulating its phosphorylation and ubiquitination, Proc. Natl. Acad. Sci. U.S.A. 111 (46) (2014) 16586–16591.
[29] J. Yu, D. Zhang, J. Liu, J. Li, Y. Yu, X.R. Wu, C. Huang, RhoGDI SUMOylation at Lys-138 increases its binding activity to Rho GTPase and its inhibiting cancer cell motility, J. Biol. Chem. 287 (17) (2012) 13752–13760.
[30] A. Kirabo, S.P. Oh, H. Kasahara, K.U. Wagner, P.P. Sayeski, Vascular smooth muscle Jak 2 deletion prevents angiotensin II-mediated neointima formation following injury in mice, J. Mol. Cell. Cardiol. 50 (6) (2011) 1026–1034.
[31] H. Hitomi, K. Kaifu, Y. Fujita, T. Sofue, D. Nakano, K. Moriwaki, T. Hara, H. Kiyomoto, M. Kohno, H. Kobori, A. Nishiyama, Angiotensin II shifts insulin signaling into vascular remodeling from glucose metabolism in vascular smooth muscle cells, Am. J. Hypertens. 24 (10) (2011) 1149–1155.
[32] M.A. Bunni, I.I. Kramarenko, L. Walker, J.R. Raymond, M.N. Garnovskaya, Role of integrins in angiotensin II induced proliferation of vascular smooth muscle cells, Am. J. Physiol. Cell Physiol. 300 (3) (2011) C647–C656.
[33] Y.J. Shen, X.X. Zhu, X. Yang, B. Jin, J.J. Lu, B. Ding, Z.S. Ding, S.H. Chen, Cardamonin inhibits angiotensin II-induced vascular smooth muscle cell proliferation and migration by downregulating p38 MAPK, Akt, and ERK phosphorylation, J. Nat. Med. 68 (3) (2014) 623–629.
[34] J.A. Moraes, A.C. Frony, A.M. Dias, M. Renovato-Martins, G. Rodrigues, C. Marcinkiewicz, J. Assreuy, C. Barja-Fidalgo, Alpha1beta1 and integrin-linked kinase interact and modulate angiotensin II effects in vascular smooth muscle cells, Atherosclerosis 243 (2) (2015) 477–485.
[35] D. Popovic, D. Vucic, I. Dikic, Ubiquitination in disease pathogenesis and treatment, Nat. Med. 20 (11) (2014) 1242–1253.
[36] Z. Li, Z. Shen, L. Du, J. He, S. Chen, J. Zhang, Y. Luan, G. Fu, Fn14 is regulated via the RhoA pathway and mediates nuclear factor-kappaB activation by Angiotensin II, Am. J. Transl. Res. 8 (12) (2016) 5386–5398.
[37] L.J. Liu, F.J. Yao, G.H. Lu, C.G. Xu, Z. Xu, K. Tang, Y.J. Cheng, X.R. Gao, S.H. Wu, The role of the Rho/ROCK pathway in AngII and TGF-β1-induced atrial remodeling, PLoS One 11 (9) (2016) e0161625.
[38] H. Xie-Zukauskasa, J. Dasa, B.L. Short, J.S. Gutkindd, P.E. Ray, Heparin inhibits Angiotensin II-induced vasoconstriction on isolated mouse mesenteric resistance arteries through Rho-Aand PKA-dependent pathways, Vasc. Pharmacol. 58 (4) (2013) 313–318.
[39] W.C. Chiu, J.M. Juang, S.N. Chang, C.K. Wu, C.T. Tasi, Y.Z. Tseng, F.T. Chiang, Angiotensin II regulates the LARG/RhoA/MYPT1 axis in rat vascular smooth muscle in vitro, Acta Pharmacol. Sin. 33 (12) (2012) 1502–1510.
[40] J.X. Yang, B. Chen, Y.Y. Pan, J. Han, F. Chen, S.J. Hu, Zoledronate attenuates angiogenic effects of angiotensin II-stimulated endothelial progenitor cells via RhoA and MAPK signaling, PLoS One 7 (10) (2012) e46511.
[41] E. Pagnin, A. Semplicini, M. Sartori, A.C. Pessina, L.A. Calò, Reduced mRNA and protein content of Rho guanine nucleotide exchange factor (RhoGEF) in Bartter's and Gitelman's Syndromes: relevance for the pathophysiology of hypertension, Am. J. Hypertens. 18 (9 Pt 1) (2005) 1200–1205.
[42] N. Moriki, M. Ito, T. Seko, Y. Kureishi, R. Okamoto, T. Nakakuki, M. Kongo, N. Isaka, K. Kaibuchi, T. Nakano, RhoA activation in vascular smooth muscle cells from stroke-prone spontaneously hypertensive rats, Hypertens. Res. 27 (4) (2004) 263–270.
[43] W. Nour-Eldine, C.M. Ghantous, K. Zibara, L. Dib, H. Issaa, H.A. Itani, N. El-Zein, A. Zeidan, Adiponectin attenuates angiotensin II-induced vascular smooth muscle cell remodeling through nitric oxide and the RhoA/ROCK pathway, Front. Pharmacol. 7 (2016) 86.
[44] F. Custodis, M. Eberl, H. Kilter, M. Bö hm, U. Laufs, Association of RhoGDIa with Rac1 GTPase mediates free radical production during myocardial hypertrophy, Cardiovasc. Res. 71 (2) (2006) 342–351.